RMetS Royal Meteorological Society
Geoscience Data Journal
Open Access
DATA PAPER

A climatology of easterly waves in the tropical Western Hemisphere

J. I. Belanger*, M. T. Jelinek and J. A. Curry

School of Earth and Atmospheric Sciences, Georgia Institute of Technology, Atlanta, GA, USA

Correspondence: J. I. Belanger, School of Earth and Atmospheric Sciences, Georgia Institute of Technology, Atlanta, GA, USA, E-mail: james.belanger@gmail.com

The U.S. Department of Commerce under NOAA Grant 3506G58 and the National Science Foundation under NSF Grant 3506G42 provided funding support. Additional funding support for JB was provided by a NSF SEES Fellowship under NSF Grant 1414868.

To understand the relationship among easterly waves, tropical cyclones (TCs), and the large-scale environment, a robust climatology of easterly waves for the tropical Western Hemisphere has been developed. The foundation for the climatology is a new easterly wave tracking algorithm that identifies westwards propagating disturbances over the tropical East Pacific, Atlantic, and Africa. To assess the issue of track dependencies and easterly wave representation, climatologies are prepared separately from the NCEP-NCAR, CFS-R, ERA-40, and ERA-Interim reanalyses. The source code for the easterly wave-tracking algorithm along with the easterly wave climatology for each atmospheric reanalysis is publicly available from NOAA's National Centers for Environmental Information.

Geosci. Data J. ***3****: 40–49 (2017), doi: 10.1002/gdj3.40*

Received: 16 May 2016, revised: 21 September 2016, accepted: 1 November 2016

Key words: atmospheric science, climate, easterly waves, tropical cyclones, hurricanes

Dataset

Identifier: doi: 10.7289/V5ZC80SX
Creator: Belanger, J. I., Jelinek, M. T., Curry, J. A.
Title: African Easterly Wave Climatology
Publisher: National Centers for Environmental Information, NESDIS, NOAA, U.S. Department of Commerce
Publication year: 2014
Resource type: Dataset
Version: 1

Introduction

Tropical easterly waves (EWs) are synoptic-scale, quasi-periodic perturbations that occur within the trade wind belt, have a horizontal wavelength typically between 2000 and 5000 km, and a preferred periodicity of 2–7 days (Carlson, 1969; Kiladis *et al.*, 2006; Burpee, 1972). EW initiation most commonly occurs over the African continent, but other genesis regions include the tropical Atlantic, Central America, and the tropical East Pacific. As approximately 60% of all Atlantic tropical cyclones including 85% of all major hurricanes originate from EWs (Agudelo *et al.*, 2011), their genesis, evolution, and variability has been the subject of active tropical dynamics research.

Hypotheses for the formation of EWs include the following: baroclinic–barotropic instabilities of an absolutely unstable African easterly jet (Burpee, 1972, 1974; Diaz and Aiyyer, 2015); transient perturbations triggered by finite-amplitude diabatic heating (Carlson, 1969; Hall *et al.*, 2006; Thorncroft *et al.*, 2008; Mekonnen *et al.*, 2006); inertial (symmetric) instability of the intertropical convergence zone (ITCZ) in regions of strong cross-equatorial pressure gradient (Toma and Webster, 2010a,b); mountain-induced lee vortices (Mozer and Zehnder, 1996a,b; Lin *et al.*, 2005) or Rossby wave breaking via North Atlantic storm track variability (Leroux *et al.*, 2011). Recently, the applicability of the baroclinic–barotropic mechanism for EW genesis over Africa has been challenged. Hall et al. (2006) showed that with realistic values of low-level damping, the African easterly jet is stable with respect to perturbations using linear normal-mode instability theory. In addition, as the longitudinal extent of the African easterly jet is approximately 40°, Thorncroft et al. (2008) argue that the African easterly jet is not capable of supporting realistic amplitudes of African EWs based on normal-mode growth rates. However, recent idealized numerical research by Diaz and Aiyyer (2015) has attempted to qualify the role of barotropic–baroclinic instability in African EW genesis. Their simulations indicate that the African easterly jet may be absolutely unstable which would allow upstream energy

fluxes via baroclinic and barotropic energy conversions to initiate new African EWs.

In the East Pacific, the origin of EWs also remains a topic of considerable debate. Earlier research indicated that these waves originate over Africa or the Caribbean and propagate into the East Pacific (Raymond *et al.*, 2006; Pasch and Avila, 1994; Frank, 1975). Recent studies (Ferreira and Schubert, 1997; Serra *et al.*, 2008; Toma and Webster, 2010a,b) have provided observational and theoretical evidence to suggest many of these waves form *in situ* in the tropical East Pacific and are generated through barotropic or inertial instability of the transient ITCZ. Absolute instability (Diaz and Aiyyer, 2015) may also have important implications for easterly wave genesis here, where barotropic or inertial instability is present and the zonal flow may be absolutely unstable.

While EW genesis continues to be an active topic of tropical dynamics research, the EW's lifecycle and evolution has practical implications for hydroclimate research and tropical hazard applications. When examined on an annual to interannual basis, EWs may provide an important link between seasonal East Pacific or North Atlantic tropical cyclone characteristics and climate teleconnection patterns including modes of Atlantic and Pacific extratropical and tropical variability. However, there is presently no publicly available observational archive for tropical EWs. Instead, previous studies that have examined the interannual variability in EWs and its relationship with large-scale climate variability have developed their own EW climatologies (Hopsch *et al.*, 2007; Thorncroft and Hodges, 2001; Agudelo *et al.*, 2011). These climatologies and resulting statistical relationships are conditionally dependent on the wave-tracking algorithm and particular atmospheric reanalysis that is used. We submit there is a need to develop a standard, open-source easterly wave climatology that will allow new climate dynamics research to be conducted and to corroborate previous research research.

The purpose of this study is to extend the previous research on easterly waves by presenting a new publicly available, easterly wave-tracking climatology for the tropical East Pacific, tropical Atlantic, and Africa called African Easterly Wave Climatology (AEWC), Version 1. An important distinction from previous work is that our tracking approach has been applied to several global atmospheric reanalyses for a variety of atmospheric vertical levels. Furthermore, the source code for the easterly wave-tracking algorithm and the EW climatology for each atmospheric reanalysis is available from NOAA's National Centers for Environmental Information.

1 Methodology

1.1. Data

Historical climatologies of easterly waves are determined for several global reanalysis datasets, including: the Climate Forecast System-Reanalysis (CFS-R; 1979–2010) (Saha *et al.*, 2010), NCEP/NCAR Reanalysis I (NCEP/NCAR 1948–2010) (Kalnay *et al.*, 1996), ECMWF Re-Analysis-Interim (ERA-Interim; 1979–2010) (Dee *et al.*, 2011), and ECMWF Re-Analysis-40 (ERA-40; 1958–2001) (Uppala *et al.*, 2005). The CFS-R and ERA-Interim datasets represent the current state of the art in terms of global reanalysis but are temporally limited to years encompassing the satellite era. Although the ERA-40 and NCEP/NCAR datasets may not be as robust, they have longer historical records and may provide a longer climatological perspective of EW variability.

The CFS-R was created using a high-resolution global model that couples the atmosphere–ocean–land surface–sea ice system and covers the period 1979 to present. The CFS-R has a 50-km (T382) horizontal resolution, includes 62 vertical levels and features the same data assimilation system, Gridpoint Statistical Interpolation, that is used in NCEP's Global Forecast System (GFS) model to generate initial conditions. In this study, the global CFS-R dataset was utilized on a geographic coordinate system using a regular latitude–longitude grid with $0.5^\circ \times 0.5^\circ$ horizontal resolution.

The NCEP/NCAR I reanalysis was constructed from a data assimilation system and model identical to the GFS model that was operational at NCEP as of January 1995, except that it was integrated at a reduced horizontal resolution of approximately 210 km (T62) with 28 vertical levels. Although this reanalysis dataset has been used extensively in global and regional large-scale atmospheric studies, there are a number of issues that have been identified including: spurious moisture and humidity data especially in the tropics, improper assimilation of upper tropospheric satellite radiances, and some periods of missing data during the period 1948 to present. A complete list of known problems with the NCEP/NCAR I reanalysis is available from NOAA's Earth System Research Laboratory (ESRL) and the Climate Prediction Center (CPC).

The ERA-40 reanalysis uses a 3D variational data assimilation technique, has a horizontal resolution of approximately 120 km (T159), and features 60 vertical levels. A number of problems have been identified in the literature since its release, including a stepwise increase in analysis quality due to new satellite radiance measurements over time, and excessive precipitation and humidity across tropical oceanic regions especially in the period since 1991 (26). A complete list of these issues is available from ECMWF.

The most recent European reanalysis, known as ERA-Interim, features the most sophisticated data assimilation system of the four reanalyses considered here – a 12-h 4D variational data assimilation system. The ERA-Interim also includes variational bias correction to better handle satellite radiance data and has a horizontal resolution of approximately 80 km (T255) with 60 vertical levels. The ERA-Interim reanalysis is produced using a version of ECMWF's Integrated Forecast System model that was operational from December 2006 to June 2007 (26). In this study, both the

global ERA-40 and ERA-Interim datasets were utilized on a geographic coordinate system using a regular latitude–longitude grid at $1.0° \times 1.0°$ horizontal resolution.

Several satellite data products are also used in constructing the EW climatologies. To determine the convective character of the easterly wave, both outgoing long-wave radiation (OLR) and cloud brightness temperatures are analysed. The Outgoing Longwave Radiation – Daily Climate Data Record – was acquired from NOAA's National Climatic Data Center for the period 1979–2010 on a $1.0° \times 1.0°$ equal-angle grid. This Climate Data Record (CDR) was originally developed by Hai-Tien Lee and colleagues for NOAA's CDR programme. OLR anomalies are calculated by removing the daily OLR from the long-term daily mean for the period 1981–2010. Cloud brightness temperatures are retrieved using the Cloud Archive User Service (CLAUS) for the period July 1983 to June 2009 (Hodges *et al.*, 2000; Robinson, 2002). In addition, a number of microwave-derived satellite products are used including: total precipitable water, rain rate, and cloud liquid water content for the period 1987–2010. The DMSP SSM/I and SSMIS data are produced by Remote Sensing Systems (www.remss.com) and sponsored by the NASA Earth Science MEaSUREs Program. The SSM/I data were taken from the following instruments and for the specified time periods: F08 (1987–1991), F10 (1990–1997), F11 (1991–2000), F13 (1995–2009), F14 (1997–2008), F15 (1999–2006), F16 (2003–2010), and F17 (2006–2010). For individuals interested in modifying or expanding the easterly wave climatology to the present, we recommend that users consider the NOAA Climate Data Record of SSM/I and SSMIS for microwave-derived satellite products.

1.2. Easterly wave-tracking algorithm

Here, we discuss the most essential components of the easterly wave-tracking algorithm. More detailed information on the wave identification and tracking methodology including how the easterly wave climatologies may be updated in real time is available in the dataset and source code readme available from NOAA (ftp://ftp.ncdc.noaa.gov/pub/data/aewc-v1/src/src_readme.docx).

1.2.1. Background

Several factors were considered before constructing the easterly wave-tracking algorithm. Fink *et al.* (2004) and Chen (2006) summarize the strengths and weakness of manual *versus* automated tracking approaches. For our purposes, the automated approach was used given the large number of years and reanalyses that were needed to be processed for EWs. Previous studies by Fink et al. (2004) and Agudelo et al. (2011) identified the EW trough using the Hovmöller method based on spatio-temporal filtered 2–6 days meridional winds and westwards-moving relative vorticity anomalies, respectively. This approach produces wave trajectories for EWs that leave Africa and move across the tropical Atlantic. Despite the technique's strong fundamentals, a number of opportunities for algorithm improvement were identified. First, this algorithm does not allow for the continuous tracking of an easterly wave once it has weakened below the tracking threshold but later strengthens. Second, this method only identifies easterly waves that pass across a particular longitude and therefore is specifically tailored to address easterly waves that move from Africa into the tropical Atlantic. This approach is not designed to track EWs that develop *in situ* in the tropical Atlantic or Caribbean or short-lived waves that form and decay over Africa. Third, the use of spatio-temporal filtered variables introduces a phase shift in the Hovmöllers of relative vorticity anomalies especially over Central America, limiting the scheme's ability to identify which EWs pass from the Atlantic into the East Pacific. In addition, the use of band-passed filtered data requires a long time series making it inappropriate for use in real-time operational wave-tracking applications. Finally, the use of relative vorticity anomalies alone makes tracking of EWs more difficult through regions where relative vorticity is dominated by background shear vorticity (e.g. the southern Caribbean).

Another wave identification routine detailed in Thorncroft and Hodges (2001) based on the Hodges (1995) tracking algorithm of relative vorticity maxima exceeding a threshold of $0.5 \times 10^{-5}\ s^{-1}$ was also considered. However, Berry *et al.* (2007) provided a more sophisticated, physically based tracking algorithm using the advection of streamfunction curvature vorticity to identify the location of ridges or troughs for a particular pressure level and time step. This method has the advantage over Agudelo et al. (2011) by objectively indicating the location of an easterly wave regardless of longitude. In addition, the method provides supplemental structural information that the Hovmöller method or the algorithm by Hodges (1995) does not provide including the meridional wavelength as well as the meridional tilt of the trough axis of the easterly wave, which can indicate whether the easterly wave is growing or decaying via baroclinic or barotropic energy conversion. However, a deficiency of the Berry et al. (2007) approach is that it does not track the easterly wave with time. Although this functionality could be added, wave identification is only one part of the easterly wave identification and tracking algorithm that we have developed. In addition, we have determined that the Berry wave identification technique has difficulty in indicating the correct trough locations in the transition region between the Atlantic and East Pacific, likely because the contribution of curvature vorticity from the background climatology is not removed prior to trough identification.

1.2.2. Data preparation and wave identification

The easterly wave climatologies are generated separately for three isobaric levels – 600, 700, and

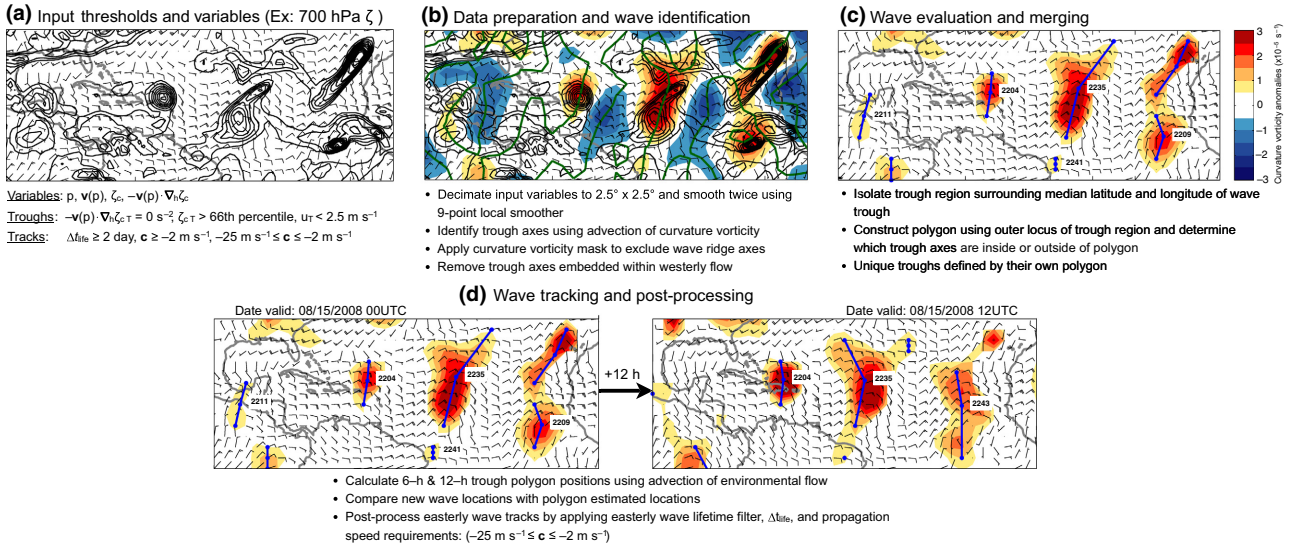

Figure 1. Schematic of the easterly wave tracking algorithm that uses horizontal winds, v(p) on an isobaric level, p, curvature vorticity anomalies, ζc(p), and the advection of curvature vorticity anomalies, $-v\nabla_h\zeta c(p)$ to identify an easterly wave trough's location. The trough thresholds include where the advection of curvature vorticity anomaly equals 0 s^{-2}, the curvature vorticity anomaly threshold is the 66th percentile of all curvature vorticity anomalies for a given reanalysis, and the zonal wind is less than 2.5 m s^{-1}. (a) Black contours denote where the 700 hPa relative vorticity is greater than 0 s^{-1}. (b) Colour-filled contours are the coarse resolution curvature vorticity anomalies and green contours denote where the advection of curvature vorticity anomalies equal 0 s^{-2}. (c) Regions where the curvature vorticity anomalies are greater than the curvature vorticity anomaly threshold (e.g., 0.50 × 10^{-5} s^{-1}) are shaded, and the blue lines denote the location of identified wave troughs. (a–c) are valid for 0000 UTC 15 August 2008. (d) Similar to (c) except shows the wave-tracking step 12 h later valid for 1200 UTC 15 August 2008. Easterly waves must have a minimum duration, Δtlife, of at least 2 days and a westwards, median propagation speed between −2 m s^{-1} and −25 m s^{-1}.

850 hPa – and require the kinematic variables on an isobaric surface, p, including: the 2D horizontal wind field, v(p); curvature vorticity anomalies, $\zeta_c(p)$; and the advection of curvature vorticity anomalies, $-v\nabla_h\zeta_c(p)$ (see Figure 1(a)). As curvature vorticity, especially in the lower troposphere, is influenced by local topography across Central America and over Africa, isobaric curvature vorticity anomalies are calculated by removing the 6-h long-term average. The 6-h climatology varies with the reanalysis product used for easterly wave identification and is defined for the temporal extent of each reanalysis (i.e. CFS-R: 1979–2010, ERA-40: 1958–2001, ERA-Interim: 1980–2010, and NCEP/NCAR Reanalysis I: 1948–2010).

Besides evaluating the kinematic variables on their native grid, coarse grids are also constructed by filtering the variables using convolution with a Gaussian filter onto a regular latitude–longitude geographic coordinate system with a horizontal resolution of 2.5° × 2.5° (see Figure 1(b)). Each variable is then smoothed twice using a 9-point local smoother, which reduces vorticity signals from mesoscale systems while retaining the synoptic-scale easterly wave structure. Easterly wave trough locations are identified in regions where the zonal wind is less than 2.5 m s^{-1}, the curvature vorticity anomaly is greater than the 66th percentile of all isobaric curvature vorticity anomalies for a given reanalysis, and the advection of curvature vorticity is equal to 0 s^{-2}.

1.2.3. Wave evaluation and merging

After identifying all easterly wave trough locations, the next step is to ensure that the delineated trough locations correspond to unique EWs. Through recursion, each trough axis is compared to its neighbouring trough axes to determine whether a trough axis belongs to the same wave. This wave-merging step uses the median latitude and longitude of the wave axis to isolate the locus of points that exceed the wave trough minimum curvature vorticity anomaly threshold. However, if the latitudinal or longitudinal extent of the isolated region is in excess of 25°, then the curvature vorticity threshold to define the wave trough region is increased by 50% until the enclosed region is smaller than 25°. Next, a polygon is constructed using the outer locus of selected points. Then, the median latitude and longitude coordinates for each trough axis are compared to a particular trough axis polygon to determine if these coordinates lie inside or outside of the polygon. Any trough axis that is located within the polygon enclosing the wave trough is defined as belonging to the same easterly wave and is merged with any other similarly identified trough axes. During the merging process, a new average latitude and longitude of the wave trough is defined which is the average of all individual median latitude and longitude trough locations as well as the latitude and longitude extent of the individual trough axes. This

process creates a new subset of merged trough axes.

An example of the wave identification and trough merging step is shown in Figure 1 for a 700 hPa easterly wave in the eastern Atlantic, just off the West Coast of Africa. In Figure 1(c), two distinct easterly wave troughs are identified by the wave-tracking algorithm (i.e. a classic African easterly wave to the south and an easterly wave from an inverted mid-latitude trough to the north). After 12 h (Figure 1(d)), the same two trough locations are identified by the algorithm, but due to their proximity, it is determined that these troughs now belong to the same easterly wave and hence are denoted by a single trough axis.

1.2.4. Wave tracking and post-processing for wave characteristics

After wave merging is complete, the next step is the wave-tracking phase, where the algorithm identifies which of the current set of identified EWs were present at previous time steps. Various strategies were tested to increase the efficiency of wave tracking between time steps. The final approach assumes that the easterly wave's propagation is governed to first order by the mean environmental advection on an isobaric surface. For each time step, a polygonal search area is created for the next 6-h and 12-h based on the spatial extent of the wave trough, its current propagation speed, and the mean environmental winds of the wave trough region. These polygons are used to identify which waves identified at the current time step are located within a wave's polygonal search area from the previous 6-h or 12-h time step. If no match is found, then the algorithm assumes the identified easterly wave is a new wave.

Once wave tracking is complete, the easterly wave dataset undergoes additional post-processing. The algorithm requires that all EWs have a minimum lifetime, Δt_{life}, of at least 2 days and that the easterly wave has a median propagation speed, c, between -25 m s^{-1} and -2 m s^{-1}. This latter requirement is to ensure that the wave exhibits westwards propagation during most of its lifecycle.

In addition, wave characteristics describing the genesis region, kinematic and thermodynamic structure for each wave are collected during post-processing. Seven wave genesis regions are defined within the wave-tracking domain of 35°S–35°N, 140°W–40°E (Figure 2). After identifying the wave's genesis region, kinematic and thermodynamic characteristics are calculated using first- and second-order moments as well as other statistics based on an analysis of the easterly wave's trough region. All grid points that reside within the wave trough are considered, and for satellite datasets that are at a different resolution than the reanalysis resolution, linear interpolation is used to match the data regions. Tables 1 and 2 provide a complete list of the kinematic and satellite-derived variables that were developed for each wave, respectively.

2. Results

2.1. Annual easterly wave track density climatology

One benefit of the EW climatologies is that they may be used to generate spatial information of easterly wave characteristics. Figure 3 shows an example of one of these characteristics: the annual easterly wave track density at 700 hPa after counting the number

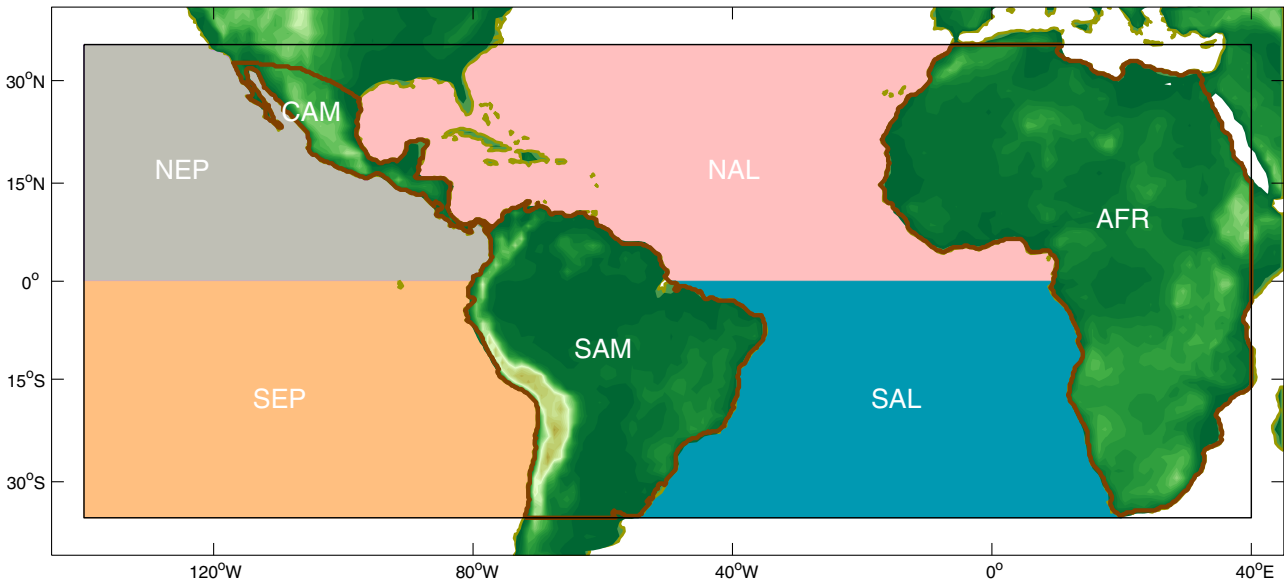

Figure 2. Map of the easterly wave-tracking domain: 35°S–35°N, 140°W–140°E along with the various wave generation regions: Northeast Pacific (NEP), Southeast Pacific (SEP), Central America (CAM), South America (Dee *et al.,* 2011), North Atlantic (NAL), South Atlantic (SAL), Africa (AFR), and along with Other (OTH), which is all other locations within the domain that is not contained within the seven defined regions.

Table 1. Kinematic variables for each easterly wave (EW) along with a description of the method that was used for its derivation.

Variables	Description
Wave observation count	Number of 6-h observations for each EW
Wave trajectory Id	Unique EW identifier
Wave time	Time stamp for EW (units: days since 1900-01-01 00:00:00)
Wave trough centroid latitude	Averaging the latitudes for all EW trough grid points
Wave trough centroid longitude	Averaging the longitudes for all EW trough grid points
Wave trough maximum latitude	Finding the maximum latitude for all EW trough grid points
Mean longitude of wave trough maximum latitude	Averaging the longitudes of all EW trough maximum latitude grid points
Wave trough minimum latitude	Finding the minimum latitude for all EW trough grid points
Mean longitude of wave trough minimum latitude	Averaging the longitudes of all EW trough minimum latitude grid points
Wavelength	Horizontal wavelength of the EW (in km), using a factor four scaling of the horizontal extent of the wave trough region in the direction of the EW's forward motion
Wave trough mean relative vorticity	Averaging the relative vorticity of all EW trough grid points
Wave trough maximum relative vorticity	Finding the maximum relative vorticity of all EW trough grid points
Wave trough minimum relative vorticity	Finding the minimum relative vorticity of all EW trough grid points
Wave trough standard deviation relative vorticity	Finding the standard deviation of relative vorticity of all EW trough grid points
Wave trough mean curvature vorticity	Averaging the curvature vorticity of all EW trough grid points
Wave trough maximum curvature vorticity	Finding the maximum curvature vorticity of all EW trough grid points
Wave trough minimum curvature vorticity	Finding the minimum curvature vorticity of all EW trough grid points
Wave trough standard deviation curvature vorticity	Finding the standard deviation of curvature vorticity of all EW trough grid points
Wave trough mean shear vorticity	Averaging the shear vorticity of all EW trough grid points
Wave trough maximum shear vorticity	Finding the maximum shear vorticity of all EW trough grid points
Wave trough minimum shear vorticity	Finding the minimum shear vorticity of all EW trough grid points
Wave trough standard deviation shear vorticity	Finding the standard deviation of shear vorticity of all EW trough grid points

of easterly waves that pass over a $1^\circ \times 1^\circ$ regular latitude–longitude grid for the tracking domain 35°S–35°N × 140°W–40°E. Instead of calculating the track density using the EW's centroid location and some distance threshold, a polygon is constructed based on a 5° buffer around each easterly wave trough axis (horizontal wavelength ~2000 km), increasing the track density's representativeness. As seen in Figure 3, depending upon the reanalysis considered, there can be large differences in the average spatial structure and the number of easterly waves that pass across a particular location, once again highlighting the motivation of this study to develop several EW climatologies. Although some of this variability may be due to differences in the resolution of the reanalyses, the magnitude and spatial extent of the differences raise interesting questions on how easterly waves are represented in each reanalysis including systematic differences in the strength of the waves geographically.

According to Figure 3, African EW initiation north of the equator tends to occur farther west in the ERA-Interim and ERA-40 reanalyses relative to the CFS-R and follows the wave guide of the African easterly jet across western Africa and through the eastern tropical Atlantic. The increasing EW track density from western Africa into the tropical North Atlantic indicates that a variety of EW genesis mechanisms may be important to explain the total annual EW frequency in this region (e.g. inverted mid-tropospheric troughs from extratropical Rossby wave breaking). Similarly, the increase in EW track density in the Northeast Pacific relative to the Caribbean as seen in the ERA-Interim, ERA-40, and CFS-R indicates that *in situ* EW genesis mechanisms may play some role in explaining the total annual EW track density in this region.

Table 2. Satellite-derived variables for each EW along with a description of the method that was used for its derivation.

Variables	Description
Wave trough mean Claus brightness temperature	Averaging the Claus brightness temperature of all EW trough grid points
Wave trough standard deviation Claus brightness temperature	Finding the standard deviation of Claus brightness temperature of all EW trough grid points
Wave trough Claus brightness temperature area fraction	Proportion of all EW trough grid points where valid Claus brightness temperature is available relative to the total number of EW trough grid points
Wave trough mean total precipitable water	Averaging the SSM/I total precipitable water, where available, of all EW trough grid points
Wave trough standard deviation total precipitable water	Finding the standard deviation of total precipitable water of all EW trough grid points
Wave trough total precipitable water area fraction	Proportion of all EW trough grid points where valid SSM/I total precipitable water is available relative to the total number of EW trough grid points
Wave trough mean rain rate	Averaging the SSM/I rain rate, where available, of all EW trough grid points
Wave trough standard deviation rain rate	Finding the standard deviation of SSM/I rain rate of all EW trough grid points
Wave trough rain rate area fraction	Proportion of all EW trough grid points where valid SSM/I rain rate is available relative to the total number of EW trough grid points
Wave trough mean cloud liquid water	Averaging the SSM/I cloud liquid water, where available, of all EW trough grid points
Wave trough standard deviation cloud liquid water	Finding the standard deviation of SSM/I cloud liquid water of all EW trough grid points
Wave trough cloud liquid water area fraction	Proportion of all EW trough grid points where valid SSM/I cloud liquid water is available relative to the total number of EW trough grid points
Wave trough mean outgoing long-wave radiation	Averaging outgoing long-wave radiation from the NCDC Daily OLR CDR of all EW trough grid points
Wave trough standard deviation outgoing long-wave radiation	Finding the standard deviation of outgoing long-wave radiation of all EW trough grid points
Wave trough outgoing long-wave radiation area fraction	Proportion of all EW trough grid points where valid outgoing long-wave radiation is available relative to the total number of EW trough grid points
Wave trough mean outgoing long-wave radiation anomaly	Averaging OLR anomalies of all EW trough grid points. OLR anomalies derived using a daily 30-year OLR climatology for the period 1981–2010.
Wave trough standard deviation outgoing long-wave radiation anomaly	Finding the standard deviation of OLR anomalies of all EW trough grid points. OLR anomalies derived using a daily 30-year OLR climatology for the period 1981–2010.

These results are in agreement with the recent findings by Serra et al. (2008) and Toma and Webster (2010a,b) that suggests some East Pacific easterly waves generate *in situ versus* originating solely from the tropical Atlantic. The EW track density in the Southeast Pacific and South Atlantic is also of interest because less attention has been given to waves in these regions. These results differ from the climatologies of easterly waves by Roundy and Frank (2004) and Kiladis *et al.* (2009) where waves were detected using "TD-filtered" OLR or brightness temperature. From Figure 3, it remains unclear how many of the systems in the Southern Hemisphere are canonical easterly waves *versus* other types of mesoscale disturbances. Nonetheless, these systems may be important in modulating hydroclimate variability over southern Africa or South America (Cohen *et al.*, 1995) or air quality over southern Africa (Tyson *et al.*, 1996). Figure 3 shows that the region south of the Congo Basin of Africa is a preferred initiation location, as is the region downstream of the northern Andes in South America.

2.2. Accessing the AEWC dataset and source code

The easterly wave datasets for each isobaric level and reanalysis are stored in netCDF-4 format with ZLIB compression using CF-1.6 conventions. The datasets are publicly available via ftp from NOAA's National Centers for Environmental Information (ftp://ftp.ncdc.noaa.gov/pub/data/aewc-v1/data/). When using this dataset, please use the following citation: Belanger, James I., Jelinek, Mark T., Curry, Judith A. (2014): "African Easterly Wave Climatology, Version 1." NOAA National Climatic Data Center. [indicate subset used]. doi:10.7289/V5ZC80SX [Access Date].

The source code of the easterly wave-tracking algorithm including all MATLAB functions and scripts that were used in its creation is available via ftp from NOAA's National Centers for Environmental Information (ftp://ftp.ncdc.noaa.gov/pub/data/aewc-v1/src/). Although the authors do not plan to update the climatologies any further, interested users may continue to update the climatologies on their own by following the

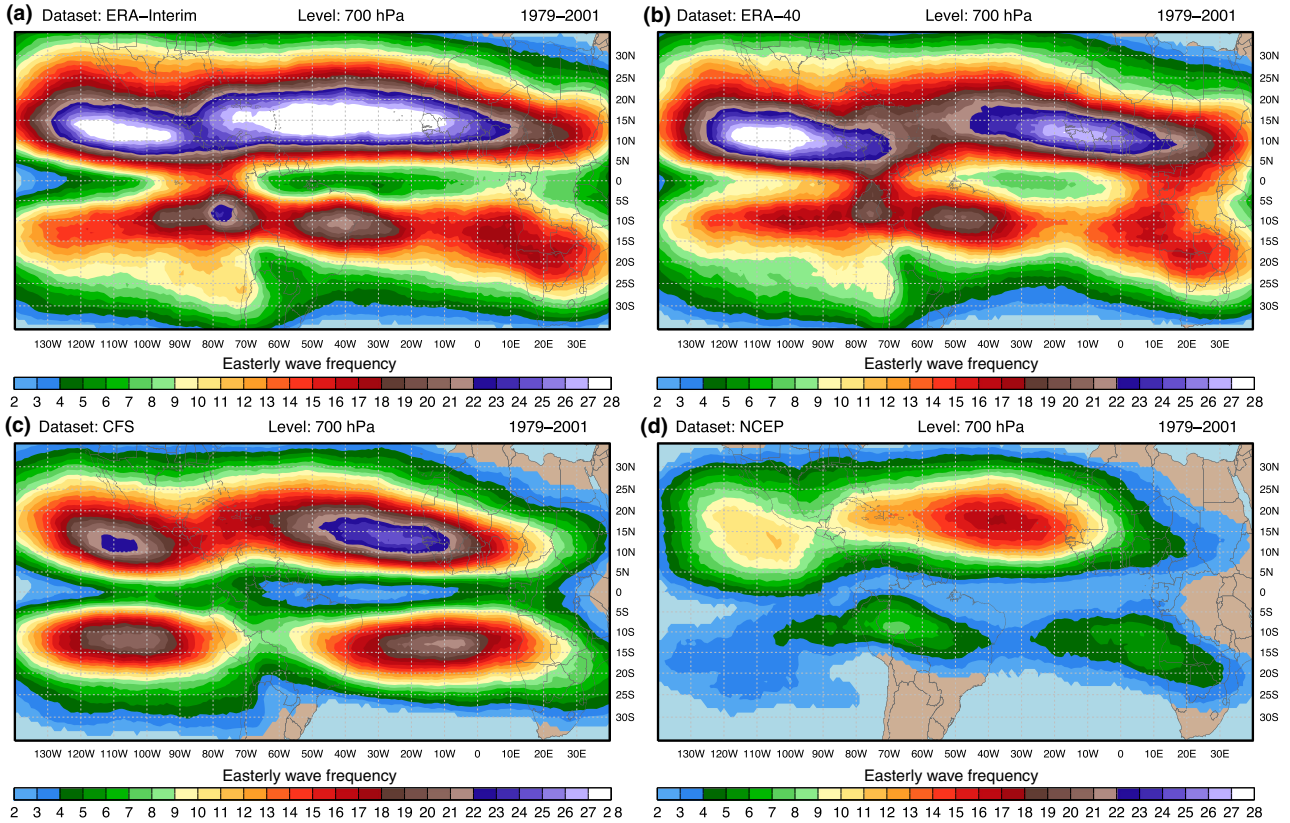

Figure 3. Annual average easterly wave track density at 700 hPa for the (a) ERA-Interim, (b) ERA-40, (c) CFS-R, and (d) NCEP/NCAR reanalysis datasets for the period 1979–2001.

readme instructions included in the source code (ftp://ftp.ncdc.noaa.gov/pub/data/aewc-v1/src/src_readme.docx).

3. Concluding remarks

In this study, easterly wave climatologies are presented for the tropical Western Hemisphere after applying a new tracking algorithm to the ERA-Interim, ERA-40, CFS-R, and NCEP-NCAR reanalyses at 600, 700, and 850 hPa using reanalysis-dependent tracking thresholds. The tracking scheme eliminates some of the deficiencies found in previous algorithms in terms of both identifying and tracking easterly waves that move across Central America and into the East Pacific, as well as ensuring that the identified and tracked waves are westwards propagating, synoptic-scale systems including canonical easterly waves. The source code for the easterly wave tracking algorithm along with the EW climatology for each atmospheric reanalysis is publicly available from NOAA's National Centers for Environmental Information. Although there are no plans to update the datasets in real time, the archived source code should allow other organizations or individuals to expand the climatology to include more recent years. In addition, the easterly wave identification and tracking algorithm may also be used as a real-time forecasting tool. In fact, Climate Forecast Applications Network (CFAN) currently produces probabilistic, ensemble EW forecasts using the ECMWF Ensemble Prediction System based on this wave-tracking algorithm. These projections may be used in conjunction with tropical cyclone genesis forecasts to quantify the risk of easterly wave-induced TC genesis in the tropical North Atlantic or East Pacific.

The easterly wave climatologies presented here are the first open-source, publicly available datasets of their kind. With these observational datasets, we envision that a number of new and previously researched topics may be explored. For instance, the datasets may be used to compare with idealized numerical simulations to uncover the principal physical mechanisms associated with easterly wave genesis and evolution, especially as the genesis mechanisms may be regionally dependent due to variable background configurations (Kiladis et al., 2006; Serra et al., 2008). In addition, further research is still needed to quantify how large-scale modes of climate variability modulate easterly waves and their regional characteristics (Martin and Thorncroft, 2015). Although climate variability may project directly onto the mean thermal and moisture structure of the atmosphere, we expect that tropical hydroclimate variability may be manifested through changing eddy characteristics of easterly waves, particularly in their frequency, intensity, or trajectory.

Acknowledgements

The authors would like to thank Paula Agudelo and Chris Thorncroft for their helpful suggestions during construction and evaluation of the easterly wave-tracking algorithm. The authors are also grateful for the feedback received by three reviewers, and for Hai-Ru Chang who assisted in data management of the various reanalyses. The U.S. Department of Commerce under NOAA Grant 3506G58 and the National Science Foundation under NSF Grant 3506G42 provided funding support for this research. Additional funding support for the PI was provided by a NSF SEES Fellowship under NSF Grant 1414868.

References

Agudelo P, Hoyos C, Curry J, Webster P. 2011. Probabilistic discrimination between large-scale environments of intensifying and decaying African easterly waves. *Climate Dynamics* **36**: 1379–1401. doi:10.1007/s00382-010-0851-x.

Belanger JI, Jelinek MT, Curry JA. 2014. African Easterly Wave Climatology. National Centers for Environmental Information, NESDIS, NOAA, U.S. Department of Commerce, doi:10.7289/V5ZC80SX.

Berry G, Thorncroft C, Hewson T. 2007. African easterly waves during 2004—analysis using objective techniques. *Monthly Weather Review* **135**: 1251–1267, doi:10.1175/MWR3343.1.

Burpee RW. 1972. The origin and structure of easterly waves in the lower troposphere of North Africa. *Journal of the Atmospheric Sciences* **29**: 77–90, doi:10.1175/1520-0469(1972)029<0077:TOASOE>2.0.CO;2.

Burpee RW. 1974. Characteristics of North African easterly waves during the summers of 1968 and 1969. *Journal of the Atmospheric Sciences* **31**: 1556–1570, doi:10.1175/1520-0469(1974)031<1556:CONAEW>2.0.CO;2.

Carlson TN. 1969. Synoptic histories of three African disturbances that developed into Atlantic hurricanes. *Monthly Weather Review* **97**: 256–276, doi:10.1175/1520-0493(1969)097<0256:SHOTAD>2.3.CO;2.

Chen T-C. 2006. Characteristics of African easterly waves depicted by ECMWF reanalyses for 1991–2000. *Monthly Weather Review* **134**: 3539–3566, doi:10.1175/MWR3259.1.

Cohen JCP, Silva Dias MAF, Nobre CA. 1995. Environmental conditions associated with Amazonian squall lines: a case study. *Monthly Weather Review* **123**: 3163–3174, doi:10.1175/1520-0493(1995)123<3163:ECAWAS>2.0.CO;2.

Dee DP, Uppala SM, Simmons AJ, Berrisford P, Poli P, Kobayashi S, Andrae U, Balmaseda MA, Balsamo G, Bauer P, Bechtold P, Beljaars ACM, van de Berg L, Bidlot J, Bormann N, Delsol C, Dragani R, Fuentes M, Geer AJ, Haimberger L, Healy SB, Hersbach H, Hólm EV, Isaksen L, Källberg P, Köhler M, Matricardi M, McNally AP, Monge-Sanz BM, Morcrette JJ, Park BK, Peubey C, de Rosnay P, Tavolato C, Thépaut JN, Vitart F. 2011. The ERA-Interim reanalysis: configuration and performance of the data assimilation system. *Quarterly Journal of the Royal Meteorological Society* **137**: 553–597, doi:10.1002/qj.828.

Diaz M, Aiyyer A. 2015. Absolute and convective instability of the African easterly jet. *Journal of the Atmospheric Sciences* **72**: 1805–1826, doi:10.1175/JAS-D-14-0128.1.

Ferreira RN, Schubert WH. 1997. Barotropic aspects of ITCZ breakdown. *Journal of the Atmospheric Sciences* **54**: 261–285, doi:10.1175/1520-0469(1997)054<0261:BAOIB>2.0.CO;2.

Fink AH, Vincent DG, Reiner PM, Speth P. 2004. Mean state and wave disturbances during phases I, II, and III of GATE based on ERA-40. *Monthly Weather Review* **132**: 1661–1683, doi:10.1175/1520-0493(2004)132<1661:MSAWDD>2.0.CO;2.

Frank NL. 1975. Atlantic tropical systems of 1974. *Monthly Weather Review* **103**: 294–300, doi:10.1175/1520-0493(1975)103<0294:ATSO&gt2.0.CO;2.

Hall NMJ, Kiladis GN, Thorncroft CD. 2006. Three-dimensional structure and dynamics of African easterly waves. part II: dynamical modes. *Journal of the Atmospheric Sciences* **63**: 2231–2245, doi:10.1175/JAS3742.1.

Hodges KI. 1995. Feature tracking on the unit sphere. *Monthly Weather Review* **123**: 3458–3465, doi:10.1175/1520-0493(1995)123<3458:FTOTUS>2.0.CO;2.

Hodges KI, Chappell DW, Robinson GJ, Yang G. 2000. An improved algorithm for generating global window brightness temperatures from multiple satellite infrared imagery. *Journal of Atmospheric and Oceanic Technology* **17**: 1296–1312, doi:10.1175/1520-0426(2000)017<1296:AIAFGG&gt2.0.CO;2.

Hopsch SB, Thorncroft CD, Hodges K, Aiyyer A. 2007. West African storm tracks and their relationship to Atlantic tropical cyclones. *Journal of Climate* **20**: 2468–2483, doi:10.1175/JCLI4139.1.

Kalnay E, Kanamitsu M, Kistler R, Collins W, Deaven D, Gandin L, Iredell M, Saha S, White G, Woollen J, Zhu Y, Leetmaa A, Reynolds R, Chelliah M, Ebisuzaki W, Higgins W, Janowiak J, Mo KC, Ropelewski C, Wang J, Jenne R, Joseph D. 1996. The NCEP/NCAR 40-year reanalysis project. *Bulletin of the American Meteorological Society* **77**: 437–471, doi:10.1175/1520-0477(1996)077<0437:TNYRP>2.0.CO;2.

Kiladis GN, Thorncroft CD, Hall NMJ. 2006. Three-dimensional structure and dynamics of African easterly waves. part I: observations. *Journal of the Atmospheric Sciences* **63**: 2212–2230, doi:10.1175/JAS3741.1.

Kiladis GN, Wheeler MC, Haertel PT, Straub KH, Roudy PE. 2009. Convectively coupled equatorial waves. *Review of Geophysics* **47**: RG2003, doi:10.1029/2008RG000266.

Leroux S, Hall NMJ, Kiladis GN. 2011. Intermittent African easterly wave activity in a dry atmospheric model: influence of the extratropics. *Journal of Climate* **24**: 5378–5396, doi:10.1175/JCLI-D-11-00049.1.

Lin Y-L, Robertson KE, Hill CM. 2005. Origin and propagation of a disturbance associated with an African easterly wave as a precursor of hurricane Alberto (2000). *Monthly Weather Review* **133**: 3276–3298, doi:10.1175/MWR3035.1.

Martin ER, Thorncroft C. 2015. Representation of African easterly waves in CMIP5 models. *Journal of Climate* **28**: 7702–7715, doi:10.1175/JCLI-D-15-0145.1.

Mekonnen A, Thorncroft CD, Aiyyer AR. 2006. Analysis of convection and its association with African easterly waves. *Journal of Climate* **19**: 5405–5421, doi:10.1175/JCLI3920.1.

Mozer JB, Zehnder JA. 1996a. Lee vorticity production by large-scale tropical mountain ranges. part II: a mechanism for the production of African waves. *Journal of the Atmospheric Sciences* **53**: 539–549, doi:10.1175/1520-0469(1996)053<0539:LVPBLS>2.0.CO;2.

Mozer JB, Zehnder JA. 1996b. Lee vorticity production by large-scale tropical mountain ranges. part I: eastern North Pacific tropical cyclogenesis. *Journal of the Atmospheric Sciences* **53**: 521–538, doi:10.1175/1520-0469(1996)053<0521:LVPBLS>2.0.CO;2.

Pasch RJ, Avila LA. 1994. Atlantic tropical systems of 1992. *Monthly Weather Review* **122**: 539–548, doi:10.1175/1520-0493(1994)122<0539:ATSO>2.0.CO;2.

Raymond DJ, Bretherton CS, Molinari J. 2006. Dynamics of the intertropical convergence zone of the East Pacific. *Journal of the Atmospheric Sciences* **63**: 582–597, doi:10.1175/JAS3642.1.

Robinson G. 2002. Long Time Series of Global Thermal Infra-red Imagery of the Earth as part of the Cloud Archive User Service (CLAUS) Project. NCAS British Atmospheric Data Centre. Dataset.

Roundy P, Frank W. 2004. A climatology of waves in the equatorial region. *Journal of the Atmospheric Sciences* **61**: 2105–2132, doi:10.1175/1520-0469(2004)061<2105:ACOWIT>2.0.CO;2.

Saha S, Moorthi S, Pan H-L, Wu X, Wang J, Nadiga S, Tripp P, Kistler R, Woollen J, Behringer D, Liu H, Stokes D, Grumbine R, Gayno G, Wang J, Hou Y-T, Chuang H-Y, Juang H-MH, Sela J, Iredell M, Treadon R, Kleist D, Van Delst P, Keyser D, Derber J, Ek M, Meng J, Wei H, Yang R, Lord S, Van Den Dool H, Kumar A, Wang W, Long C, Chelliah M, Xue Y, Huang B, Schemm J-K, Ebisuzaki W, Lin R, Xie P, Chen M, Zhou S, Higgins W, Zou C-Z, Liu Q, Chen Y, Han Y, Cucurull L, Reynolds RW, Rutledge G, Goldberg M. 2010. The NCEP climate forecast system reanalysis. *Bulletin of the American Meteorological Society* **91**: 1015–1057, doi:10.1175/2010BAMS3001.1.

Serra YL, Kiladis GN, Cronin MF. 2008. Horizontal and vertical structure of easterly waves in the Pacific ITCZ. *Journal of the Atmospheric Sciences* **65**: 1266–1284, doi:10.1175/2007JAS2341.1.

Thorncroft C, Hodges K. 2001. African easterly wave variability and its relationship to Atlantic tropical cyclone activity. *Journal of Climate* **14**: 1166–1179, doi:10.1175/1520-0442(2001)014<1166:AEWVAI>2.0.CO;2.

Thorncroft CD, Hall NMJ, Kiladis GN. 2008. Three-dimensional structure and dynamics of African easterly waves. part III: genesis. *Journal of the Atmospheric Sciences* **65**: 3596–3607, doi:10.1175/2008JAS2575.1.

Toma V, Webster P. 2010a. Oscillations of the intertropical convergence zone and the genesis of easterly waves part II: numerical verification. *Climate Dynamics* **34**: 605–613, doi:10.1007/s00382-009-0585-9.

Toma V, Webster P. 2010b. Oscillations of the intertropical convergence zone and the genesis of easterly waves. part I: diagnostics and theory. *Climate Dynamics* **34**: 587–604, doi:10.1007/s00382-009-0584-x.

Tyson PD, Garstang M, Swap R, Kâllberg P, Edwards M. 1996. An air transport climatology for subtropical southern Africa. *International Journal of Climatology* **16**: 265–291, doi:10.1002/(SICI)1097-0088(199603)16:3<265:AID-JOC8>3.0.CO;2-M.

Uppala SM, KÅllberg PW, Simmons AJ, Andrae U, Bechtold VDC, Fiorino M, Gibson JK, Haseler J, Hernandez A, Kelly GA, Li X, Onogi K, Saarinen S, Sokka N, Allan RP, Andersson E, Arpe K, Balmaseda MA, Beljaars ACM, Berg LVD, Bidlot J, Bormann N, Caires S, Chevallier F, Dethof A, Dragosavac M, Fisher M, Fuentes M, Hagemann S, Hólm E, Hoskins BJ, Isaksen L, Janssen PAEM, Jenne R, McNally AP, Mahfouf JF, Morcrette JJ, Rayner NA, Saunders RW, Simon P, Sterl A, Trenberth KE, Untch A, Vasiljevic D, Viterbo P, Woollen J. 2005. The ERA-40 re-analysis. *Quarterly Journal of the Royal Meteorological Society* **131**: 2961–3012, doi:10.1256/qj.04.176.